Deep-Sea Research II ∎ (∎∎∎∎) ∎∎∎–∎∎∎

Contents lists available at ScienceDirect

Deep-Sea Research II

journal homepage: www.elsevier.com/locate/dsr2

Multi-decadal variability and trends in the El Niño-Southern Oscillation and tropical Pacific fisheries implications

D.E. Harrison [a,*], Andrew M. Chiodi [a,b]

[a] NOAA Pacific Marine Environmental Laboratory, 7600 Sand Point Way NE, Seattle, WA 98115, USA
[b] Joint Institute for the Study of the Ocean and Atmosphere, University of Washington, Seattle, WA 98195, USA

ARTICLE INFO

Keywords:
ENSO
Decadal
Multi-decadal
Variability
Trend
Statistical significance

ABSTRACT

Extremes of the El Niño-Southern Oscillation (ENSO) are known to have various socio-economic impacts, including effects on several Pacific fisheries. The 137-year-long record of Darwin sea-level pressure offers a uniquely long-term perspective on ENSO and provides important insight into various aspects of interannual to century-scale variability that affects these fisheries. One particular issue of interest is whether there is a centennial-scale (or longer) trend that can be expected to alter the future distributions of these fisheries. Since most tropical Pacific fishery records are no longer than a few decades, another issue is the extent to which trends over these recent decades are a good basis for detecting the presence of long-term (e.g., centennial-scale) deterministic changes, and perhaps thereby projecting future conditions. We find that the full 137-yr trend cannot be distinguished from zero with 95% confidence, and also that the ENSO variance in recent decades is very similar to that of the early decades of the record, suggesting that ENSO has not fundamentally changed over the period of large increase in atmospheric CO_2. However, the strong multi-decadal variability in ENSO is reflected in decades with quite different levels of ENSO effects on the ecosystem. Many multi-decadal subsets of the full record have statistically significant trends, using standard analysis techniques. These multi-decadal trends are not; however, representative of the record-length trend, nor are they a useful basis for projecting conditions in subsequent decades. Trend statistical significance is not a robust foundation for speculation about the future. We illustrate how the difficulties involved in determining whether a trend is statistically significant or not mean that, even after careful consideration, an unexpectedly large number of trends may reach standard statistical significance levels over the time spans for which many newer records are available, but still not continue into future decades or be indicative of deterministic changes to the system. Analysis of the Southern Oscillation Index, another common ENSO index, but one that has been directly measured for fewer years than has Darwin, yields similar results.

1. Introduction

The warm (El Niño) and cool (La Niña) phases of the El Niño-Southern Oscillation (ENSO) are now well known to cause extremes in temperature and precipitation in affected areas around the globe (see Ropelewski and Halpert, 1987, 1989; Halpert and Ropelewski, 1992, for seminal studies on this topic, and Chiodi and Harrison, 2013, for an updated U.S. perspective). They can also cause large-scale changes in the distribution of several pelagic fish populations (Fiedler, 2002; Lehodey et al., 2006). These changes include an at least temporary collapse of the Peruvian anchovy population during some strong El Niño years (Barber and Chavez, 1983, 1986; see also Bertrand et al., 2004), links to various aspects of northeast Pacific ecosystem variability (McGowan et al., 1998), as well as dramatic changes in the distributions of Pacific tuna, especially the tropical skipjack (*Katsuwonus pelamis*) species (Kimura et al., 1997; Lehodey et al., 1997, 2006; Lu et al., 2001). Different upper-ocean changes associated with ENSO have been used to rationalize the ENSO effects on these fisheries. Among the more conspicuous are the observed basin-scale changes in the distributions of warm water, thermocline and mixed layer depth, and chlorophyll concentration along the equatorial Pacific. Zonal displacements of typical conditions extend over thousands of kilometers along the equator during ENSO extremes, and chlorophyll and sea surface temperature (SST) often track each other closely (see Fig. 1 and Park et al., 2011). Very large changes in large-scale tropical Pacific chlorophyll concentration and distribution also exist between warm and cold extremes (see Lehodey et al., 1997; Murtugudde et al., 1999; Fig. 2). In the tropical Pacific, these interannual ENSO changes have

* Corresponding author. Tel.: +1 206 526 6225.
E-mail address: D.E.Harrison@noaa.gov (D.E. Harrison).

0967-0645/$ - see front matter © 2014 Published by Elsevier Ltd.
http://dx.doi.org/10.1016/j.dsr2.2013.12.020

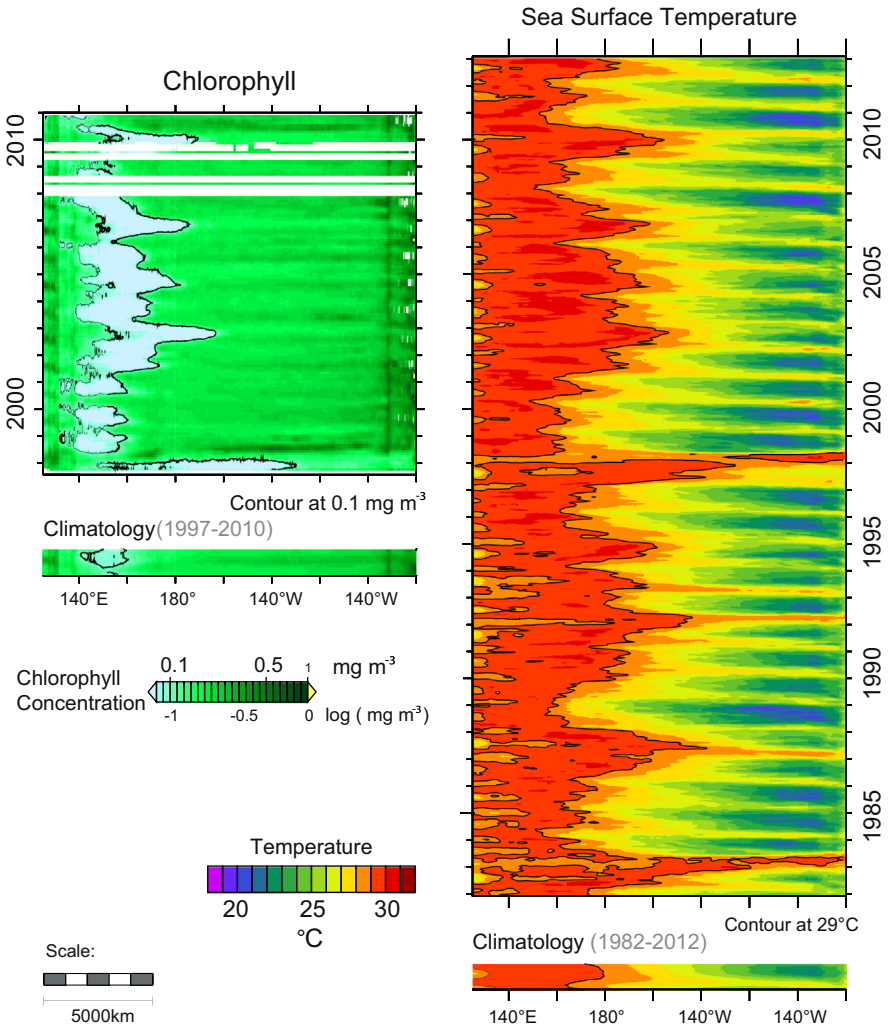

Fig. 1. Time-longitude sections of equatorial Pacific (2°S–2°N average) chlorophyll concentration (left) and sea surface temperature (right).

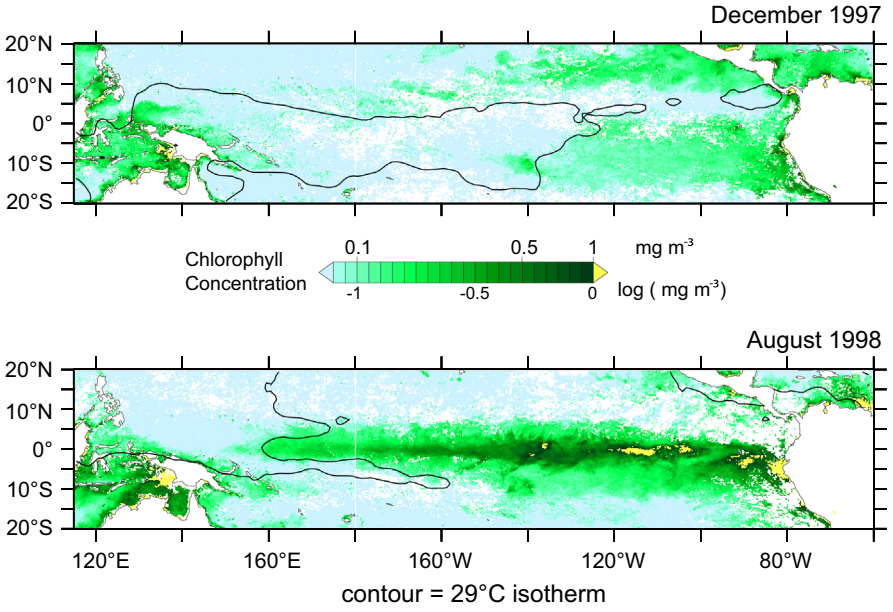

Fig. 2. Snapshots of monthly average chlorophyll conditions during the 1997–1998 transition from a strong El Niño (upper panel) to La Niña (lower panel) state. The 29 °C contour is overdrawn for reference.

Please cite this article as: Harrison, D.E., Chiodi, A.M., Multi-decadal variability and trends in the El Niño-Southern Oscillation and tropical Pacific fisheries implications. Deep-Sea Res. II (2014), http://dx.doi.org/10.1016/j.dsr2.2013.12.020

amplitudes that greatly exceed those associated with the mean seasonal cycle (see Fig. 2) or with model projections of thermal conditions over the several coming decades under increasing atmospheric CO_2 concentration. Bio-physical modeling efforts have suggested that in addition to the observed large-scale displacement of stocks associated with these changes, ENSO can have important effects on tuna recruitment and abundance statistics as well (Lehodey, 2001, 2003).

ENSO effects are thus of fundamental concern to the design and implementation of effective management practices for many of the region's fisheries (Aqorau, 2009; Miller, 2007), which, in the case of the Pacific tuna fishery, provide about 70% of the world's harvest (Lehodey et al., 1997) and are an important source of food security and economic development for the Pacific island countries and territories (Bell et al., 2012). For those affected or otherwise interested in the state of Pacific fisheries, there is reason to be very interested in how the distribution of ENSO events will change in coming decades.

There has been much interest recently in analyzing coupled Earth System models (i.e. ocean-atmosphere-land) forced with projected concentrations of atmospheric CO_2 for projections of how Earth's climate and ecosystems (including pelagic) might change in the future (Bell et al., 2012, 2013; Ganachaud et al., 2012; Lehodey et al., 2012). Although there are some relevant aspects of the projected changes that most models agree upon (e.g. sign of long-term temperature change) changes to the frequency and amplitude of ENSO is not one of them (Ganachaud et al., 2012); different models currently give decidedly different projections of how ENSO might change in the future (Collins et al., 2010; Vecchi et al., 2008). Other studies have found these models capable of displaying quite different types of interannual behavior from one multi-decadal period to the next, even when the model forcing is held constant (Wittenberg, 2009).

About a decade ago, there was vigorous debate about whether or not secular change in ENSO was already evident in the observed Darwin record; Trenberth and Hoar (1996) presented the case for this view, whereas Harrison and Larkin (1997) and Rajagopalan et al. (1997) showed that the answer depended on the choice of statistical methods (see also Trenberth and Hoar, 1997; Wunsch, 1999). More recently, Power and Smith (2007) reported that the June–December values of the Southern Oscillation Index (SOI), along with Darwin sea level pressure (SLP) averaged over the 1977–2006 period, reached record levels that "are unlikely to have come from the same 'population' as the earlier values," leading them to suggest that "climate change" was responsible. Based on linear correlation results, Diaz et al. (2001) have suggested that there have been substantial changes in the strength of several ENSO "teleconnections" between the post-1977 and previous (1948–1977, in this case) periods, including the strength of ENSO effects on atmospheric circulation anomalies in the North Pacific. Nicholls (2008) examined the behavior of the SOI in the 50-yr period from 1958 to 2007 and found a statistically significant linear trend when averages over only some months of each year were considered; however, shifting focus to other months resulted in there being no statistically significant trend. Power and Kociuba (2011) reported that the 1876–2008 trend in Darwin SLP is statistically significant at the 90% confidence level, based on a Student's '*t*' test. Focusing on SST data from an ocean reanalysis, Ray and Giese (2012) have examined the changes in various ENSO measures (e.g. amplitude, duration, frequency) throughout this (1871–2008) period and concluded that, although there are concerns about uncertainties caused by sparse SST observations, especially in the first half of their record, there is no evidence that the changes seen (including considerable decadal variability) are caused by global warming. Subsequent examination of the model runs submitted to the WCRP Coupled Model Intercomparison Project (CMIP3) by Power and Kociuba (2011), which failed to reveal a 1977–2006 SOI anomaly in these models (on average) that was similar to the one in the observations, led them to conclude that the post-1977 SOI behavior highlighted by Power and Smith (2007), though statistically unusual, is a component of natural variability (unrelated to increasing atmospheric CO_2). We are unaware of other recent studies into the long-term variability of ENSO, particularly with applications to tropical Pacific fisheries. Because of the lack of consensus in global-coupled modeling efforts (as well as observational-statistical studies), it seems timely to revisit what the available observations can contribute to our understanding of these issues.

Here we revisit the question of whether there is evidence for a long-term (>100 yr) trend in the state of the El Niño-Southern Oscillation (ENSO), and whether 100+year-long trends (best-fit-linear) can be reliably determined from shorter (i.e. 50 yr, 40 yr, 30 yr, etc.) multi-decadal records, such as those that have been made available in recent decades by various improvements to our observing capabilities, including the increased availability of data from commercial vessels and other in situ sampling methods since WWII, the use of satellite-based observations starting in the 1980s or 1990s, as well as other improvements in our ability to observe ocean ecosystems over the last two decades (Ducklow et al., 2009). To do this, we use both the traditionally discussed SOI, which has typically been the ENSO index referred to in the pelagic studies mentioned above, as well as the record of SLP from Darwin, Australia, which is both a component of the SOI and a good proxy itself for ENSO at interannual and longer timescales (e.g. correlation with the SOI is 0.9 when a 13-month triangular filter is applied to the Darwin record). We primarily consider the Darwin record because it is a good proxy for ENSO and has been directly measured for longer than the SOI. Power and Kociuba (2011) have suggested that Darwin may become a better indicator of the east–west equatorial Pacific SLP gradient than the SOI in the coming century if the relevant aspects of the WCRP/CMIP3 model predictions prove correct. We shall show that the Darwin- and SOI-based observational results are nonetheless consistent with one another at this point.

Because it offers a simple measure of whether ENSO is changing (and it is a commonly examined measure in general), we compute the slope of the best-fit line ("trend") over the full 137-yr record (s) and determine its statistical significance using the different Monte Carlo methods. We also compute the amounts of variance seen in different multi-decadal sub-segments and inspect them for evidence of secular change. Since high-quality records of many other aspects of the tropical Pacific system (e.g. fishery catch and effort data, sea surface temperature, oxygen and chlorophyll concentration) are not available for nearly as long as the Darwin record, we also determine the likelihood of being able to infer the observed 137-yr trend from just a given decadal/multi-decadal sub-segment. Further, we examine the roles that the available statistical methods may or may not play in helping to mitigate the risks involved in using shorter sub-segments to infer information about longer term behavior and decide whether deterministic change is evident.

The importance of properly considering the effects of the way variability is distributed at low frequencies before making conclusions about whether deterministic trends are present in bio-geophysical time series has already received a considerable amount of attention (e.g. Hughes and Williams, 2010; Wunsch, 1999). Thus, we expect that a general need for caution in such efforts will already be appreciated by many readers. The case-study we offer herein, for the reasons described above, is one with particular relevance to Pacific fisheries. In it, we will examine the extent to which taking a careful approach in this case, such has been advocated for previously, should really be expected to reduce the uncertainties involved.

Please cite this article as: Harrison, D.E., Chiodi, A.M., Multi-decadal variability and trends in the El Niño-Southern Oscillation and tropical Pacific fisheries implications. Deep-Sea Res. II (2014), http://dx.doi.org/10.1016/j.dsr2.2013.12.020

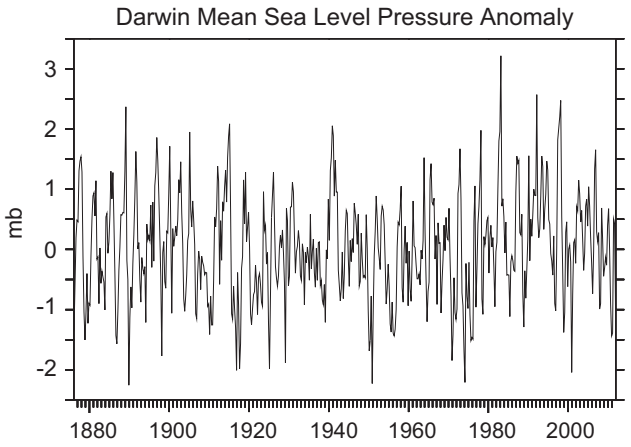

Fig. 3. Darwin seasonally averaged sea level pressure anomaly, period 1876–2011.

2. Data and methods

Monthly averaged Darwin SLP values, available from the Australian Bureau of Meteorology (BOM) at ftp://ftp.bom.gov.au/anon/home/ncc/www/sco/soi/darwinmslp.html, were averaged to seasonal resolution for this study (period 1876–2012). Tahiti SLP values were also obtained from BOM and used to calculate the SOI according to the traditional method of Troup (1965), in which case the SOI is determined from standardized Tahiti minus Darwin SLP anomalies.

The chlorophyll data shown here for illustrative purposes were obtained from the National Atmospheric and Space Administration (NASA) OceanColor website available at http://oceandata.sci.gsfc.nasa.gov/SeaWiFS (see O'Reilly et al., 1998, for discussion of the SeaWiFS chlorophyll algorithms). The National Oceanic and Atmospheric Administration (NOAA) Optimally Interpolated data set (Reynolds et al., 2002) was used for SST information (available at http://www.esrl.noaa.gov/psd/data/gridded/data.ncep.oisst.v2.html).

To determine trend statistical significance, we report mainly on results from a bootstrap/Monte Carlo-based test, such as has been available for some time now (Ephron and Tibshirani, 1991). The test procedure is as follows: (1) the record to be tested is selected; (2) the trend over this record is determined using a linear least-squares fit; (3) this trend is removed from the record so that the character of the variability that is unrelated to the trend can be estimated; (4) the amount and distribution of this variability otherwise present in the record (the non-trend variability) is evaluated; and (5) the test determines whether or not the null hypothesis that the record-length trend is produced by the non-trend variability is true. The last step in the procedure used herein involves generating a large number ($N=1000$) of model time series and comparing the distribution of these model trends with that seen in the actual record. In the bootstrap procedure, the model time series are generated by randomly sampling (with replacement) the observed detrended record, comprised of n observations each representing averages over intervals of Δt (three months in this case), spanning an overall length $T=n\Delta t$. The sub-sampling is carried out using the detrended (rather than full) record in accordance with step 3 above so that the test-estimate of the 'non-trend' behavior does not include the trend to be tested itself. In this case, n_b bootstrap samples are selected, where

$$n_b = T/T_b,$$

and T_b is the estimated time between independent samples in the original record.

For the bootstrap model, the information in step 4 listed above comes from the distribution of values seen in the actual record and the estimated value of T_b. In the base-case test used here, T_b is estimated from the lagged-autocorrelation of the record using the method proposed by Leith (1973). In this case, the lagged auto-correlation is truncated at the first zero-crossing to avoid having the answer unduly influenced by the often non-negligible long-lag auto-correlations that occur as the artifacts of using finite records.

We also discuss the character and behavior of a mixed auto-regressive moving-average (ARMA) stochastic model (Box and Jenkins, 1976). The model mainly used in this case is one with 3 auto-regressive (a_i) and 1 moving-average (b_1) parameters with the form

$$y(t) = a_1 \times y(t-1) + a_2 \times y(t-2) + a_3 \times y(t-3) + \varepsilon(t) + b_1 \times \varepsilon(t-1),$$

where $\varepsilon(t)$ is the value of a random normal process with zero mean at time t, and the parameters a_1, a_2, a_3, b_1, as well as the standard deviation of ε (σ_ε), are fit to the record in question. Over the 137 yr of record now available, we find that the best-fit ARMA(3,1) parameters (based on a minimization of the difference between the theoretical ARMA spectrum and the spectrum estimated from the actual 137-yr Darwin record) are

$$a_1 = 1.2494,\ a_2 = -0.3529,\ a_3 = -0.0935,\ b_1 = -0.6235 \quad \text{and}$$

$$\sigma_\varepsilon = 0.6463,$$

which yield the theoretical spectrum shown in Fig. 4 (red curve). The Fourier-based estimate of the spectral density of variance in the Darwin record (blue dots in Fig. 4) and its associated uncertainty are found by the methods described by Bendat and Piersol (1971).

We also briefly discuss some results from wavelet decomposition techniques described by Percival and Walden (2000). Specifically, we use the "maximal overlap discrete wavelet transform," or MODWT, employed with the LA(8) filter (as described in Chapter 5 of Percival and Walden, 2000). The MODWT allows the contribution to the total variance due to changes at a given (discrete) wavelet scale to be estimated. Generally, the MODWT wavelet scale 'j' is given by $2^{j-1}\ \Delta t$. In this case, with $\Delta t=3$ months, the first wavelet scale ($j=1$) is six months, the second ($j=2$) is one year, etc.

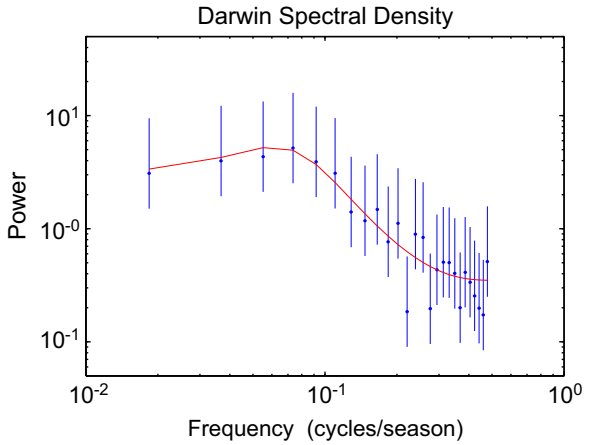

Fig. 4. Estimated spectral density of variance from the 137-yr Darwin seasonal mean sea level pressure anomaly (blue dots). The points shown represent the average over ten adjacent frequency bands, with vertical bars used to show the associated 95% confidence intervals. The red line shows the theoretical spectrum of the best-fit ARMA(3,1) stochastic model. (For interpretation of the references to color in this figure legend, the reader is referred to the web version of this article).

Please cite this article as: Harrison, D.E., Chiodi, A.M., Multi-decadal variability and trends in the El Niño-Southern Oscillation and tropical Pacific fisheries implications. Deep-Sea Res. II (2014), http://dx.doi.org/10.1016/j.dsr2.2013.12.020

3. Results

3.1. Darwin SLP variability

The seasonally averaged Darwin record is shown in Fig. 3 (period 1876–2012). Its estimated spectral density of variability is shown in Fig. 4 (blue dots), along with the estimated uncertainty (blue vertical lines) that results from averaging over ten adjacent frequency bands. The spectrum of the best-fit ARMA(3,1) model (red line) is also shown in Fig. 4. Chu and Katz (1989) have previously suggested that this class of stochastic model can be used to represent the spectral characteristics of ENSO well, and Trenberth and Hoar (1996) have previously suggested that this specific order (three auto-regressive and one moving-average parameter) is optimal for the Darwin record. Indeed, the spectra of the best-fit ARMA(3,1) model (red curve in Fig. 4) and the more traditionally estimated spectrum (blue dots) are roughly consistent with one another and agree that the Darwin, and thus ENSO, spectrum is "red" in that it is generally characterized by increased energy at longer, compared to shorter, periods.

3.2. Multi-decadal and 137 yr trends

Fig. 5 shows the best-fit linear trend over the full 137 yr, along with some examples of trends seen in some of the most recent decadal to multi-decadal sub-segments of the record. Over 100 yr, the 137-yr trend (green line) rises ~0.1 mb, or about a tenth of the time series standard deviation (0.86 mb). The trends over the last 10 and 20 yr, on the other hand, are negative and have much larger slopes (blue lines) than seen over the full 137 yr. The trend over the last 30 yr (shown by a blue line) is also negative, but sloped less steeply than those seen over the last 10 and 20 yr, whereas the trends over the last 40 and 50 yr are positively sloped (red lines). Sliding back about a decade, the sub-segment trends at these multi-decadal timescales that ended in the early 1990s to early 2000s tended to be positive (i.e. more El Niño-like) and have relatively large amplitudes (the red-dashed line shows an optimally large 50-yr case).

A similar examination of the SOI record (see companion Fig. A1 in Appendix A) shows it to be in broad agreement with Darwin in these aspects (notwithstanding the change in sign that occurs by definition).

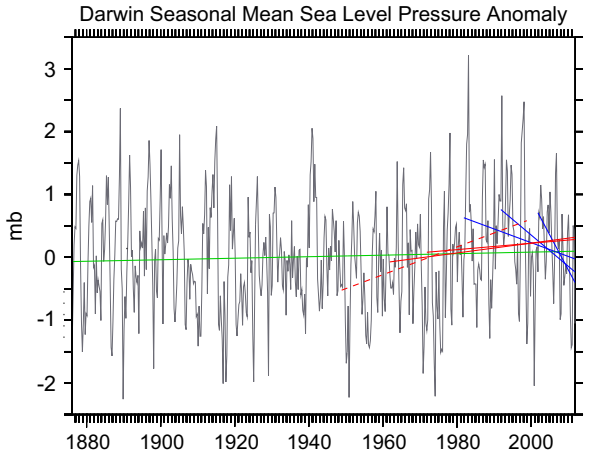

Fig. 5. Darwin seasonal sea level pressure anomaly with the best-fit trend over the full (137 yr) record (green line). Also shown are examples of best-fit trends over various decadal to multi-decadal sub-segments; trends over the last 10, 20 and 30 yr are shown in blue; the last 40 and 50 yr in red, and a 50-yr interval ending in 1998 is shown with a red dashed line. (For interpretation of the references to color in this figure legend, the reader is referred to the web version of this article).

Fig. 6 shows the distributions of trends seen in 10 to 50 yr sub-segments of the Darwin record as their starting/ending dates are methodically moved, one season at a time, through the full 137-yr record. In each panel, the 137-yr trend value is marked by a green dashed line for reference. The scale of the *x*-axis in each panel varies with the range of trend amplitudes seen, which substantially decreases moving from the shorter to longer sub-segment lengths (the entire range of trends seen in the 50-yr case fits within the middle 1/6th of the 10-yr distribution).

These distributions (Fig. 6) show that it is highly unlikely that a sub-segment start/end date selected at random would yield a trend with slope close to the best-fit 137-yr result of 7.9×10^{-5} mb/yr. In the least unlikely case (50 yr), only 8% of the sub-segment trends fall within a factor of 2 of the 137-yr value. For the shorter sub-segments considered, this is true for only 4% or fewer (see numbers in green in each panel). Most sub-segments yield trends that have considerably larger amplitudes than the one seen over the full 137 yr. The sign of these sub-segment trends; however, have a roughly equal chance of being positive or negative. For example, at 20 yr, the distribution is split perfectly between positive and negative trends (Table 1). And the largest imbalance among the segment lengths (10% more negative than positive trends at 40 yr) does not violate at standard confidence intervals the null hypothesis that positive and negative trends are equally probable according to our Monte Carlo methods. This is true also at each sub-segment length for the numbers of positive and negative trends seen in the SOI distribution (Table A1).

3.3. Trend statistical significance

Trend statistical significance tests are often used in studies like this to evaluate whether or not the trend (i.e. slope of the best-fit line) observed over a given record can easily be produced by the non-trend (e.g. interannual timescale) variability present. In the case that the observed behavior is easily matched by a model with no change in its expected average value from the beginning to the end of the record, then the observed trend is said to be not statistically significant, or statistically indistinguishable from zero. Each test discussed here agrees that the best-fit 137-yr trend (green line in Fig. 5) is not statistically significant (not statistically different from zero).

Despite this, many of the trends seen over just a few to several decades' worth of observations do reach statistical significance at the 95% confidence interval. The numbers of statistically significant trends found at each sub-segment-window length considered is shown by the shading (red for the base-case bootstrap test) in Fig. 6. None of the sub-segments that yield a trend close to the observed 137-yr trend (e.g. in the same bin) are found to be statistically significant. The statistically significant trends are instead found near the tails of the distributions (consistent with the finding that the 137-yr trend is not much different from zero).

Thus, with the benefit of a longer (137 yr) record, we can see that the statistically significant multi-decadal sub-segment trends ("pseudo-false-positives" hereafter) would, in fact, yield the most misleading estimates of the observed 137 yr trend. For records like these, predicting future behavior based on trends seen over a few decades of observations would be unwise. Yet, when longer-term perspectives like this are unavailable, it is often assumed that trends that reach statistical significance over several decades are indicative of some type of persistent change in the dynamics of the system. Test confidence intervals are used in tests like these to judge the likelihood that statistical significance is reached falsely. We next examine the reliability of test confidence intervals in the present context.

Please cite this article as: Harrison, D.E., Chiodi, A.M., Multi-decadal variability and trends in the El Niño-Southern Oscillation and tropical Pacific fisheries implications. Deep-Sea Res. II (2014), http://dx.doi.org/10.1016/j.dsr2.2013.12.020

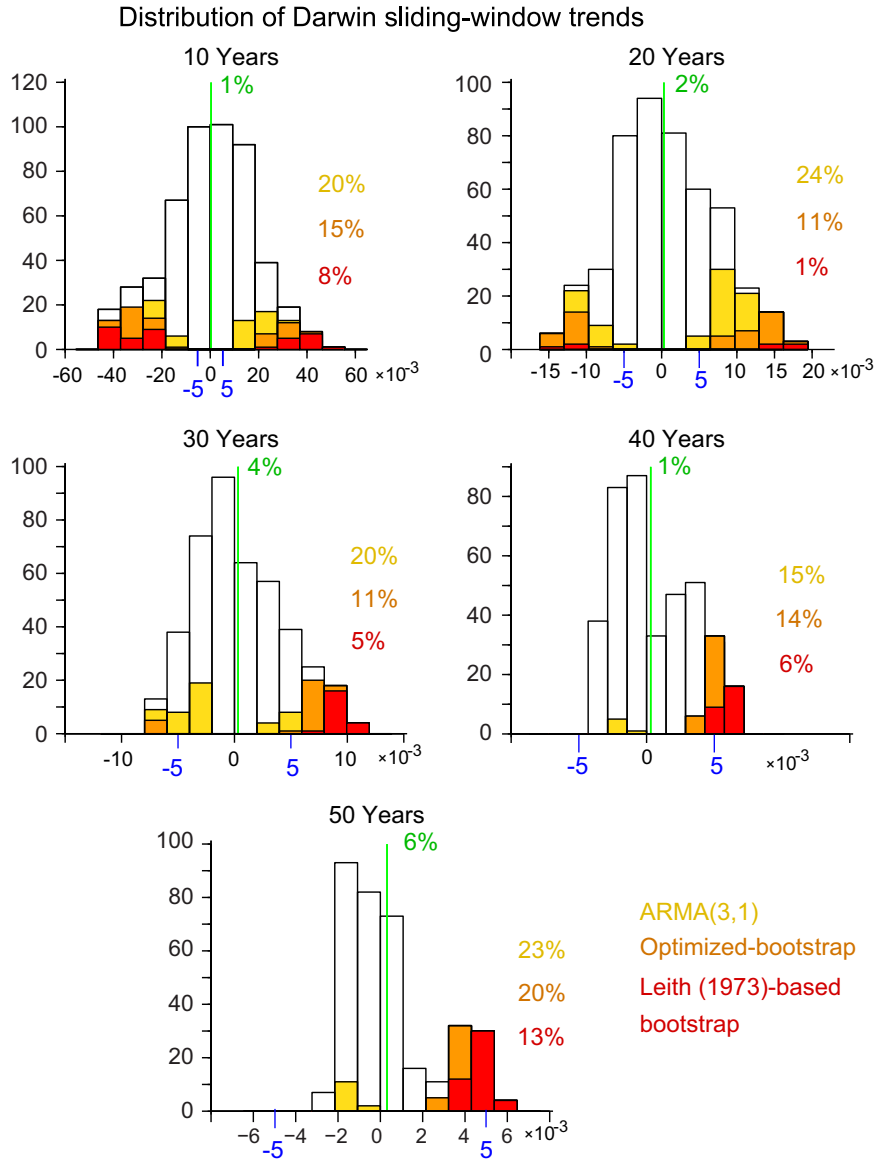

Fig. 6. Distribution of trends seen in sliding-window Darwin sub-segments of 10, 20, 30, 40, and 50 yr (period 1876–2012). Red shading shows the numbers of statistically significant trends in each bin, based on the base-case statistical methods. Red numbers list the percentage of such trends. For reference, the green line marks the location of the 137-yr best-fit trend, and the green numbers give the percentage of sub-segments that yield trends with slope within a factor of two of the 137-yr trend value. (For interpretation of the references to color in this figure legend, the reader is referred to the web version of this article).

3.4. Test reliability

For an ideal test, the nominal confidence interval gives the frequency that false-positive results are returned. For example, at 95% confidence, 5% of the results should be false-positives (null hypothesis is judged false by test, but actually true). In Fig. 6 we see that, depending on the sub-segment length, the fraction of sub-segment trends that reach statistical significance range from ~1% at 20 yr to 13% at 50 yr, or about 2.5 times more than expected if there is no long-term trend.

A simulation experiment was conducted to evaluate the test performance in a scenario where the actual spectrum and long-term trend of the (simulated) record in question are both known perfectly. The details of this simulation are provided in Appendix B, for interested readers, with the main results described below. Because the 137-yr Darwin trend is small (not statistically different from zero) we focus on the case where the spectral characteristics of the non-trend variability are realistic, but there is no specified trend.

When the base-case test is evaluated in this situation, we find that it is overly strict. For example, only 2% of the simulated 50-yr sub-segments are found to produce statistically significant trends, meaning that the test's nominal 95% confidence interval is effectively acting like a 98% confidence interval.

Next we "correct" the test so that it produces accurate results in the simulation experiment. Then we re-apply the test to the actual Darwin record. Based on the "corrected" test, we find that 11–20% of the Darwin sub-segments have statistically significant trends (Fig. 6). This is roughly 2 to 4 times as many as should be found if there is no long-term trend. The 137-yr trend, however, remains firmly insignificant (even at the nominal 66% level) according to the "corrected" test, even though we have made the test more lenient.

What is notable here is that the base-case and "corrected" tests yield substantially different numbers of statistically significant results even though the two test-assumed levels of non-trend, low-frequency variability present in Darwin both fit well within the uncertainty bounds associated with our ability to estimate

Please cite this article as: Harrison, D.E., Chiodi, A.M., Multi-decadal variability and trends in the El Niño-Southern Oscillation and tropical Pacific fisheries implications. Deep-Sea Res. II (2014), http://dx.doi.org/10.1016/j.dsr2.2013.12.020

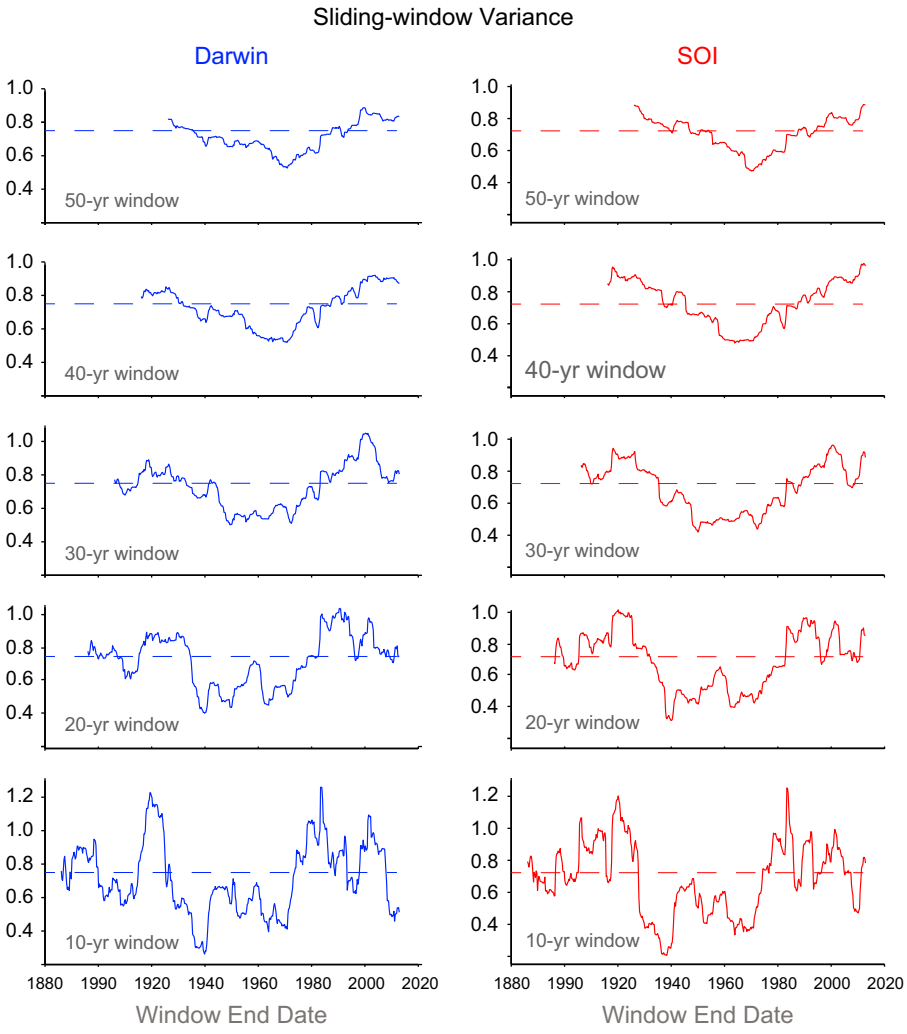

Fig. 7. Variance in sliding-window sub-segments of the Darwin (left) and SOI (right) records. The dashed line in each panel shows the average variance over all times considered.

this non-trend variability (this is described in more detail in Appendix B). Obtaining reliable confidence intervals in tests like these is difficult; when we "corrected" the test as carefully as we could based on the 137 yr of data available, the number of pseudo-false positive trends only increased.

Subsequently, we have modified the test so that it makes different assumptions about the levels of non-trend variability present at low frequency in the Darwin record that more fully sample the uncertainties associated with our ability to estimate this quantity from the actual Darwin record. Using the uncertainty bars shown in Fig. 4 to estimate this uncertainty range, we find that the pseudo-false-positive rate (at the nominal 95% interval) ranges from 0–5% in the upper-extreme to 30–45% in the lower extreme. In other words, up to 9 times too many pseudo-false-positive trends are found in the actual Darwin sub-segments, even though test assumptions remain consistent with observations to within the associated uncertainty.

This uncertainty (i.e. the nominal 95% confidence level is effectively somewhere in the 55% to $>99.9\%$ range) occurs even though we use the full 137 yr of observations and average over 10 adjacent frequency bands to constrain it (not averaging over 10 adjacent bands would result in a substantially larger uncertainty bar). Having only a single multi-decadal sub-segment available would be much more problematic. Further, the actual structure of the non-trend variability that lies beyond the lowest resolved frequency ($1/n\Delta t$) is a key aspect that can only be guessed at. It must be recognized that the outcomes of these tests greatly depend upon the necessary assumptions about the amount and character of non-trend variability present at low frequency.

We have examined the performance of other types of available tests, including those based on the now classic Student's '*t*' methods, as well as others that employ subsequent ARMA-based procedures in place of the bootstrap methods described above (the ARMA(3,1)-based test results are shown in orange shading in Fig. 8). The description of these results is provided in more detail for interested readers in Appendix B, where it can be seen that, in each case, test results show a strong sensitivity to the details of the necessary assumptions about the amount and character of low-frequency variability present.

3.5. Sliding-window variance

We have also computed the amounts of variance seen in sub-segments of the Darwin record as their starting/ending dates are moved through the full 137 yr record. The left-hand panels of Fig. 7 show the variance amounts for Darwin sub-segment lengths from 10 to 50 yr (SOI-based results are shown on the right). The overall range of sub-segment variances seen in these panels increases moving from longer to shorter sub-segments, but in each case, some of the lowest variances are seen among sub-segments that end roughly in the middle of the available historical record (1940s to 1960s). Interestingly,

Please cite this article as: Harrison, D.E., Chiodi, A.M., Multi-decadal variability and trends in the El Niño-Southern Oscillation and tropical Pacific fisheries implications. Deep-Sea Res. II (2014), http://dx.doi.org/10.1016/j.dsr2.2013.12.020

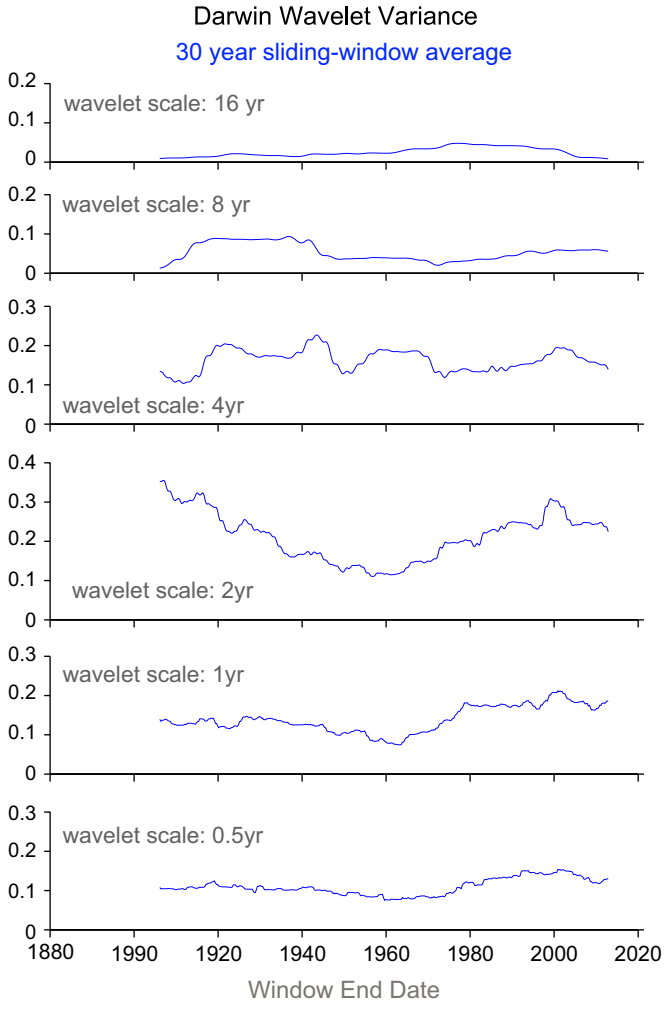

Fig. 8. Wavelet decomposition of the amounts of variance in 30-yr sliding-window sub-segments of the Darwin record.

Table 1
Numbers of positive and negative trends seen in the sliding-window sub-segments that fit within the full 137 yr Darwin record.

Sub-segment length (yr)	# positive trends	# negative trends
10	263	245
20	234	234
30	207	221
40	180	208
50	166	182

Table A1
Numbers of positive and negative trends seen in the sliding-window sub-segments that fit within the full 137 yr SOI record.

Sub-segment length (yr)	# positive trends	# negative trends
10	247	261
20	239	229
30	220	208
40	188	200
50	175	173

the variances of the longer sub-segments considered (50 and 40 yr) increase almost monotonically from this mid-record low to the start/end. In these longer multi-decadal cases, it is not difficult to imagine that consideration of just one or the other halves of the full record, in the event one portion of the record was not available, would yield misleading expectations about the trajectory of the other. The behavior at shorter sub-segment lengths (10 and 20 yr) shows also that variance generally increases moving away from the mid-point of the record and, moving forward in time, peaks in the 1980s or 1990s but then falls to near or below average levels in the most recent decades. For each sub-segment length shown, early period (pre-1940) peaks can be found with amplitudes similar to those seen in more recent decades, suggesting that long-term changes in the dynamics of the tropical Pacific are not necessary to explain the presence of either extreme. ENSO variance in recent decades is not different from that of early decades in the record.

Wavelet analysis techniques (Percival and Walden, 2000) allow the total variance contained in a record to be separated into amounts contributed by changes over different "wavelet scales." To further examine some of the decadal variability evident in Fig. 7, we have first performed wavelet decomposition (Percival and Walden, 2000) on the Darwin record. Then, just as is done for the actual Darwin record in Fig. 7, the amounts of variance at each wavelet scale are averaged in a sliding-window sense and plotted in Fig. 8. Just the 30-yr sliding-window sub-segment length is used in this case for brevity (c.f. Fig. 7 middle-row, left column). We use the same *y*-axis scale in each panel of Fig. 8 to facilitate comparison among results at different wavelet scales. It can thereby be seen that changes occurring at the 2-yr wavelet scale exhibit the largest range of 30-yr-averaged variance levels, and thus, make the largest contributions to the changes in (total) variance seen from one 30-yr sub-segment to another. As the wavelet scale moves away from 2 yr, these contributions generally decrease. Thus, most of the changes in Darwin variance from one 30-yr period to another, including the progression from high levels of variance in the early 1900s to lower levels in the 1940s to the 1960s, and then a return to high levels again in the early 2000s, are attributable to SLP changes taking place over timescales associated with the life cycle of ENSO events (Larkin and Harrison, 2002).

4. Discussion and conclusions

ENSO induces very strong interannual and multi-decadal variability in the ecosystem of the tropical Pacific Ocean, with large effects on several commercially important fisheries. Whether ENSO statistics are undergoing long-term change or are likely to change in coming decades is thus of substantial societal relevance to the communities that depend upon and are tasked with managing these fisheries (Rossig et al., 2004). We have examined the longest high-quality, directly observed ENSO index time series for insight into ENSO-related variability and change in these ecosystems and fisheries.

Over the full-record length (137 yr for Darwin) we find that the trend in Darwin SLP or Troup SOI is not statistically significant. We also find that the levels of variance seen in recent decades closely match those seen in some earlier periods, which is consistent with the SST-reanalysis-based findings of Ray and Giese (2012). Relative to these ENSO measures and over this century-long period, ENSO appears to be a stationary but quite "red" phenomenon. The planetary increase in CO_2 over this period does not seem to have induced any clear changes in ENSO.

However, there is much multi-decadal variability in ENSO. The middle decades of this period experienced less ENSO variability than did the early decades and the final decades. And some decades experienced stronger events than others. We show here that the amount of multi-decadal energy in the spectrum of

Please cite this article as: Harrison, D.E., Chiodi, A.M., Multi-decadal variability and trends in the El Niño-Southern Oscillation and tropical Pacific fisheries implications. Deep-Sea Res. II (2014), http://dx.doi.org/10.1016/j.dsr2.2013.12.020

Darwin SLP or Troup SOI makes them sufficiently "red" to severely limit the utility of information from a particular multi-decadal period (e.g. the satellite era) to project the behavior of subsequent decades, or to usefully represent the full-record length (137 yr for Darwin) trend. This suggests that for ecosystems and fisheries strongly affected by ENSO, projecting future conditions based on a few recent decades would be unwise.

Broadly speaking, there is a growing interest in examining the available multi-decadal ecosystem and fishery records for the effects of long-term climate change (Doney et al., 2012). Our results illustrate some difficulties involved in such efforts. We have shown that multi-decadal periods with large trends, whether positive or negative, often pass stringent tests of trend significance even though the full-length trend (which in the Darwin SLP case spans much of the time of rapidly increasing atmospheric CO_2) is not statistically different from zero, even with the most lenient test we have applied. In most cases, direct ecosystem and fishery observations are not available over comparably long times (Ducklow et al., 2009) so estimating long-term trends from available records must respect these uncertainties. As many others have noted (e.g. Wunsch, 1999, and references therein), red spectral time series pose very serious challenges for detecting longer term climate trends. We have shown that the risk of encountering false-positive results could easily be much higher than previously realized, even if a careful approach is taken.

It has long been recognized that individual ENSO events exhibit a range of characteristic anomaly patterns (e.g. Rasmusson and Carpenter, 1982). In the review process, the recent interest in classifying some ENSO events (particularly El Niño events) differently than others for the purposes of identifying ENSO impacts was raised. In such efforts, it should be recognized that not all regions that experience ENSO impacts are influenced by ENSO via the same pathways. In the case of the pelagic tropical Pacific ecosystem (e.g. tropical Pacific tuna fishery), the effects of ENSO are closely related to the surface marine variables used to monitor ENSO state itself (see Introduction). The range of tropical Pacific surface marine anomalies seen during the individual ENSO events forms a rather continuous, or Gaussian-like, distribution (Chiodi and Harrison, 2010; Giese and Ray, 2011). Further, it is not clear that different mechanisms need to be invoked to explain the range of SST anomaly behavior seen in the central and eastern tropical Pacific during recent El Niño events (Harrison and Chiodi, 2009). In this situation, it is difficult to see the utility of classifying El Niño events differently for the purposes of identifying their impacts on the tropical Pacific pelagic ecosystem. In other affected regions, different situations are possible. Notably, outgoing-longwave-radiation (OLR) based ENSO indices that have recently been identified exhibit a unique type of behavior (relative to the commonly used surface-marine ENSO indices) and a much closer relationship to ENSO-type atmospheric circulation anomalies over the North Pacific (among other regions) than is available from the commonly used ENSO indices. Dynamically, OLR is more closely linked than SST or SLP to the tropical Pacific atmospheric heating anomalies that cause ENSO to influence the extra-tropical atmosphere. For ecosystems affected by these extra-tropical anomalies, using the unique perspective available from observations of OLR over the tropical Pacific (Chiodi and Harrison, 2013) may prove directly useful to efforts to identify and predict (especially in the case of wintertime forecasting efforts) ENSO effects there.

The magnitude of ENSO variability is so strong that it will likely dominate environmental conditions in the tropical Pacific in the next few decades, particularly compared to the "climate change" changes that are projected by most coupled earth system models. Fishery management decisions will have to be made in a context of very substantial uncertainty about upcoming environmental conditions with large interannual and decadal variability.

Acknowledgments

This publication is [partially] funded by the Joint Institute for the Study of the Atmosphere and Ocean (JISAO) under NOAA Cooperative Agreement NA10OAR4320148, and by support from the Climate Observations Division of the NOAA Climate Program Office as well as from NOAA's Pacific Marine Environmental Laboratory. This is JISAO Contribution no. 2067, and NOAA Pacific Marine Environmental Laboratory Contribution no. 3943. We thank Dr. Phil Jones for sharing data and helpful comment, Dr. Nick Bond for helpful discussion, the anonymous reviewers for helpful comments and S. Bigley for proof-reading the manuscript.

Appendix A

The complementary figure and table provided in this appendix are produced by the methods described in the main text, except based in this case on the Southern Oscillation Index (SOI) rather than the Darwin SLP record.

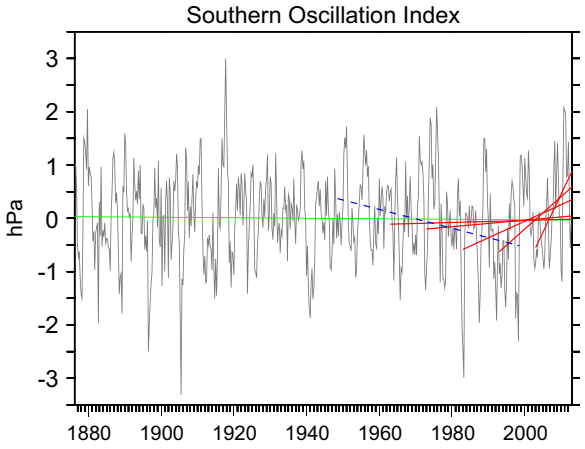

Fig. A1. As in Fig. 5, except for the Southern Oscillation Index (SOI).

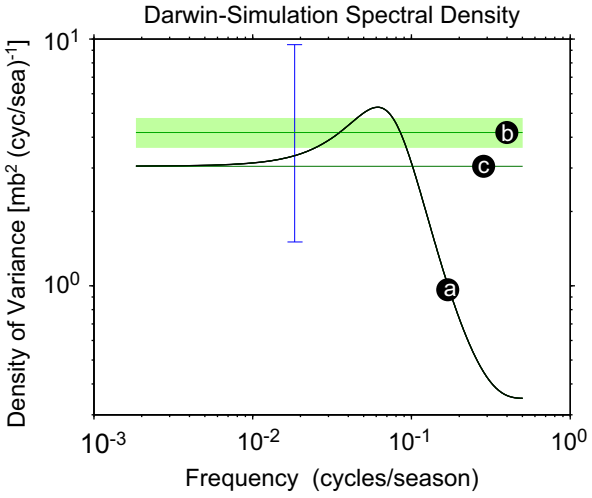

Fig. B1. Shown here are the theoretical spectrum of the ARMA(3,1) model with coefficients derived from a fit to the 137 yr of Darwin SLP observations (curve "a"), the mean test-estimated density of variance from the base-case bootstrap test (line "b"), along with the range of base-case test-estimates (green shading shows the 5th and 95th percentile; $N=1000$) seen in a simulation experiment based on synthetic 50 yr subsegments generated by the best-fit ARMA(3,1) model. Line "c" shows the value of the mean bootstrap test-estimate after being "corrected" (matched to curve "a" at low frequency). In this "corrected" mode the test returns the correct number of false-positive results. (For interpretation of the references to color in this figure legend, the reader is referred to the web version of this article.)

Please cite this article as: Harrison, D.E., Chiodi, A.M., Multi-decadal variability and trends in the El Niño-Southern Oscillation and tropical Pacific fisheries implications. Deep-Sea Res. II (2014), http://dx.doi.org/10.1016/j.dsr2.2013.12.020

Appendix B

This appendix describes the simulation experiment that was conducted to evaluate the trend statistical significance test performance in a scenario where the actual spectrum and long-term trend of the (simulated) record in question are both known perfectly. To do this, we repeatedly generated synthetic sub-segments using an ARMA(3,1) model run with the parameters derived from the fit to the full Darwin record, and then tested these synthetic sub-segments for trend statistical significance. In this case, the model is stationary and no long-term trend has been added so an ideal test should find false-positive results (indicate trend statistical significance) at a rate given by the nominal confidence interval of the test.

It is useful to illustrate this situation in frequency space. The spectrum of the ARMA(3,1) simulated 50 yr sub-segments (based on the same parameters as seen in Fig. 4) as well as the amount of non-trend variability estimated by the test in its base-case mode is shown in Fig. B1 (curve "a" and line "b", respectively). The test-estimate shown here can be understood as the spectrum of the modeled variability that the test uses to determine the distribution of trends misleadingly produced by the non-trend variability. The critical slope that must be exceeded in order for a best-fit trend to reach statistical significance is determined from this distribution.

The bootstrap test, due to its reliance on sub-sampling, effectively models a white spectrum, which in this case overestimates the simulated record's density of variance at high frequency and underestimates it at low frequency (the model estimated density of variance in this case depends on the total variance in the original record and the estimated value of T_b). That an overly strict result is seen in the simulation experiment described above is consistent with the fact that the simulated low-frequency variance is underestimated by the test (c.f. curve "a" and line "b" in Fig. B1). Indeed, we find that when the test is modified (original degrees of

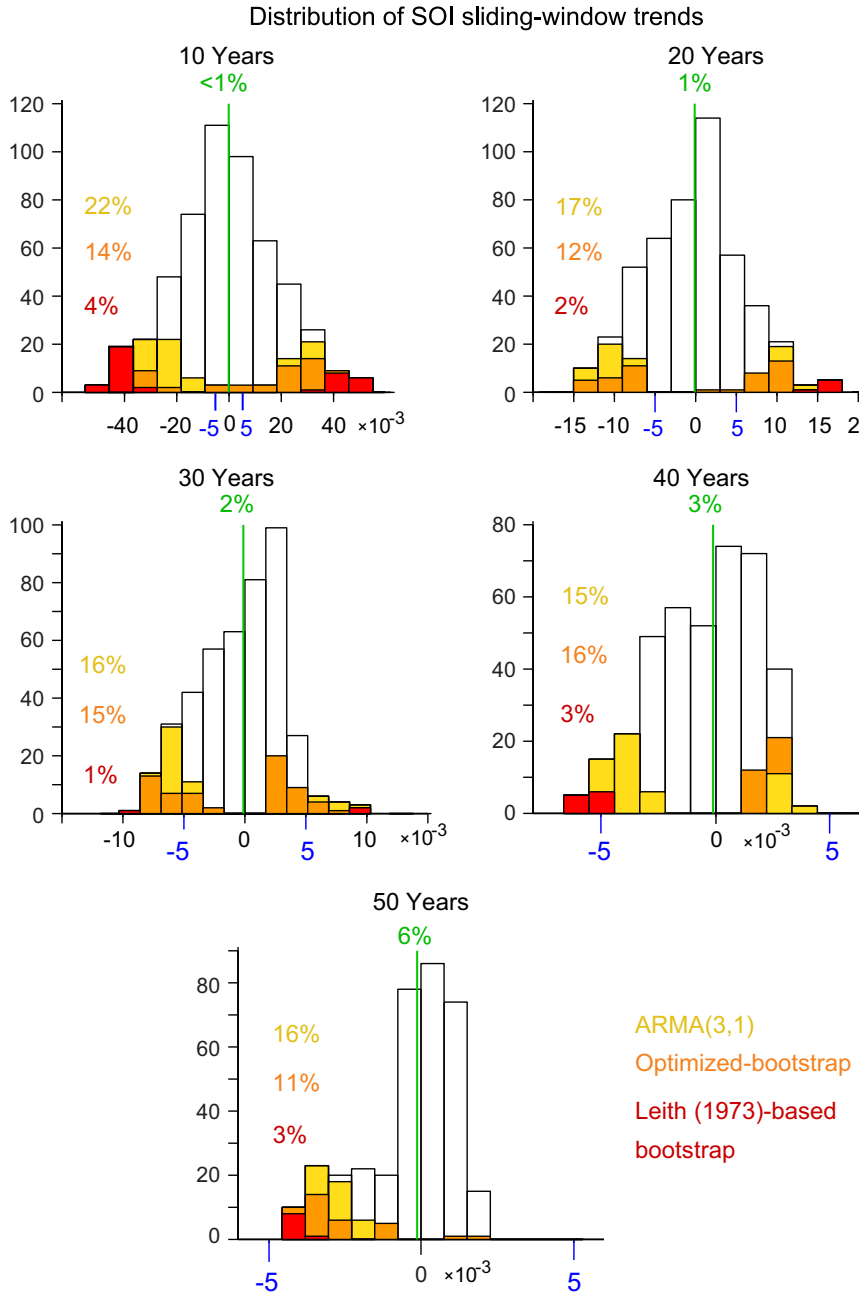

Fig. B2. As in Fig. 6, except for the Southern Oscillation Index (SOI).

freedom increased by 1/3rd) such that the test-estimated amount of non-trend variability matches the specified low-frequency ARMA(3,1) value (c.f. Fig. B1 curve "a" and line "c"), the test then returns about the correct number of false-positive results in the simulation experiment (e.g. ~5% at 95% confidence, based on 50-yr simulated sub-segments); if the best-fit ARMA(3,1) model perfectly represents the behavior of Darwin SLP, then the test is now accurate at this length scale. This modification constitutes the "corrected" bootstrap test discussed in the main text.

To examine the test performance under different assumptions about the amounts of low-frequency (non-trend) variability present, the estimated degrees of freedom can be adjusted iteratively such that the test-estimate of low-frequency variability present spans the desired range of assumptions, that is, the uncertainty associated with our ability to estimate the spectral density of variance at low frequency.

The extent of the lowest-frequency uncertainty bar shown in Fig. 4 gives a conservative estimate of this uncertainty. We find that when the bootstrap test is modified so that it assumes non-trend low-frequency variance at the upper limit of this uncertainty range, the pseudo-false-positive rate for tests conducted at the nominal 95% confidence level on the actual Darwin sub-segments ranges from 0 to 5%, depending on the sub-segment length considered. Assuming the lower limit, the pseudo-false-positive rate instead ranges from 30 to 45%, or in other words, the test returns 6 to 9 times too many false-positives.

We have repeated the analysis described here using a Student's "*t*" test as well as an ARMA(3,1) trend-significance test, in which case the three auto-regressive and one moving-average parameters are found from a fit to the individual sub-segments. We find that the "*t*" test results (not shown) are very close to (within 1% of) the bootstrap results provided that the same methods for estimating the number of degrees of freedom are used in each. This is not surprising since the "*t*"-test assumption of a normal distribution is basically consistent with the behavior of the commonly used ENSO indices (Chiodi and Harrison, 2010). The

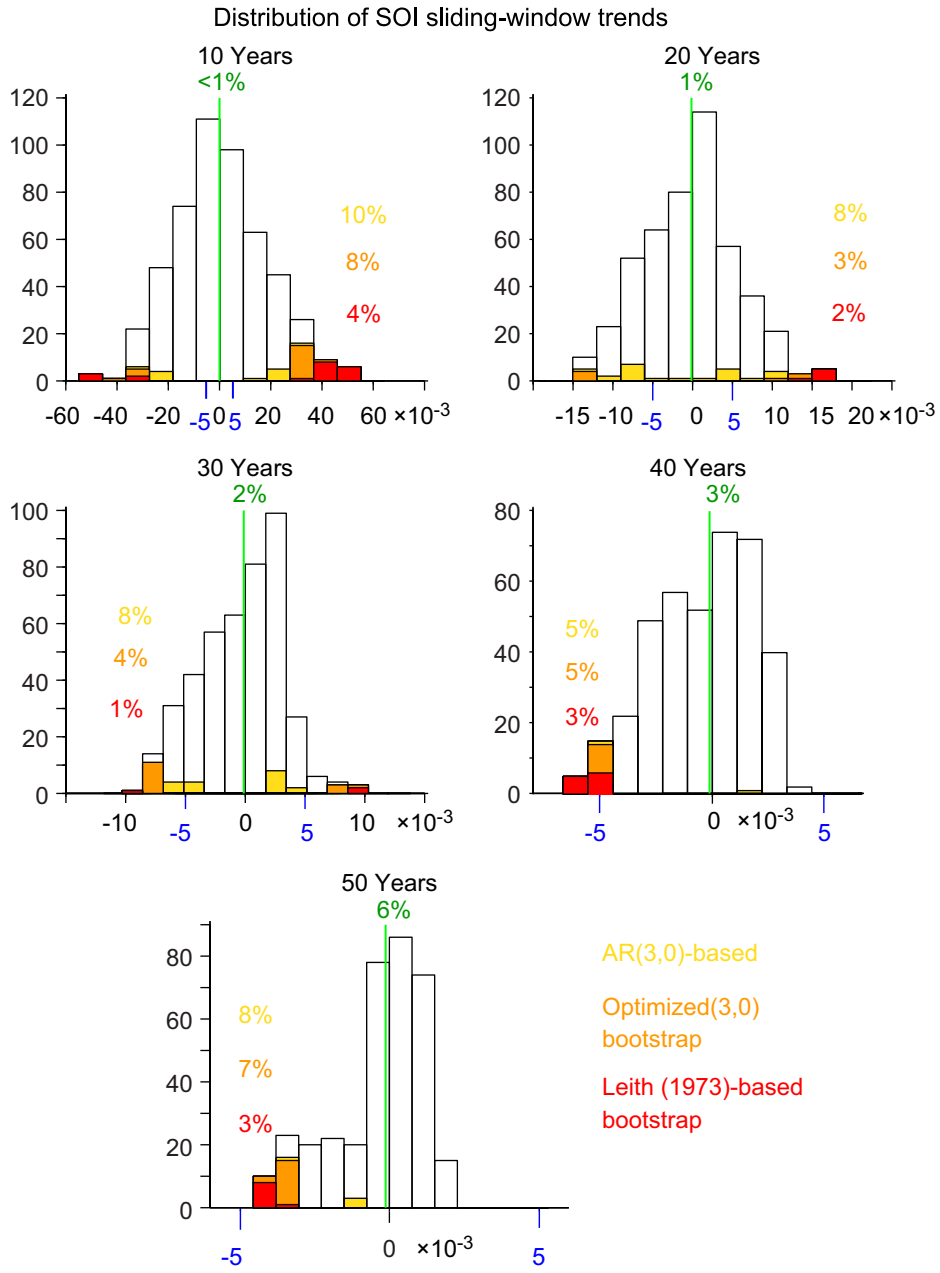

Fig. B3. As in Fig. B2, except for an AR(3,0) model form.

Please cite this article as: Harrison, D.E., Chiodi, A.M., Multi-decadal variability and trends in the El Niño-Southern Oscillation and tropical Pacific fisheries implications. Deep-Sea Res. II (2014), http://dx.doi.org/10.1016/j.dsr2.2013.12.020

ARMA(3,1) test, however, as discussed in the main test, tends to yield more statistically significant results than the optimized-bootstrap test when used in the same scenario. We attribute this increased tendency for finding statistical significance to the fact that the range of ARMA(3,1)-estimated low-frequency variability, which depends on the estimated value of five parameters in the ARMA(3-1) case, is considerably larger than in the bootstrap case (shown by the green shading in Fig. B1), which requires only one estimated parameter (T_b).

We have performed a companion study on SOI, which replicates that described above except that the Darwin record is replaced by the SOI. The results are shown in Appendix Fig. B2, and reveal that, like in the Darwin case, the base-case bootstrap test finds fewer (1 to 4%) statistically significant sub-segment trends than do the optimized-bootstrap (11–16%) and ARMA(3,1)-only tests (16–22%). We have confirmed that, as in the Darwin case, this is because the base-case bootstrap estimates of the amounts of low-frequency variability contained in SOI tend to exceed those produced by the optimized-bootstrap and ARMA (3,1)-only tests (thus making it harder for a given trend to be found statistically significant).

Using a different selection criteria than Trenberth and Hoar (1996), Chu and Katz (1985) have previously chosen the ARMA (3,0) form of model as an optimal fit to SOI. Following Chu and Katz (1985), we have also repeated the SOI trend statistical significance analysis discussed above using an ARMA(3,0) rather than ARMA(3,1) form. The results are shown in Appendix Fig. B3, and reveal that the choice of model form can have substantial effects on the ARMA-dependent (i.e. the optimized-bootstrap and ARMA-only) trend significance test results. Moving from the ARMA (3,1) to the ARMA(3,0) model in this case substantially reduces (up to a factor of 4) the number of statistically significant trends that are found in the ARMA(3,0) case compared with the ARMA(3,1) case (c.f. Figs. B2 and B3). Comparison of the test-estimated spectra (not shown, for brevity) reveals that the (non-trend) low-frequency variance levels assumed by the ARMA(3,0)-test tend to exceed those of the ARMA(3,1)-test in this case. We have confirmed that this discrepancy occurs even though both types of ARMA-estimated SOI spectra fit well within the uncertainty bounds associated with our ability to determine the amounts of the low-frequency variability in ENSO (e.g. Fig. 4). This underscores the importance that seemingly small changes in the assumed amounts of non-trend low-frequency variability can have on test outcomes.

References

Aqorau, T., 2009. Recent developments in Pacific tuna fisheries: the Palau Arrangement and the vessel day scheme. Int. J. Mar. Coast 24, 557–581Law 24, 557–581.

Barber, R.T., Chavez, F.P., 1983. Biological consequences of El Niño. Science 222, 1203–1210.

Barber, R.T., Chavez, F.P., 1986. Ocean variability in relation to living resources during the 1982–1983 El Niño. Nature 319, 279–285.

Bell, J.D., Reid, C., Batty, M.J., Lehodey, P., Rodwell, L., Hobday, A.J., Johnson, J.E., Demmke, A., 2012. Effects of climate change on oceanic fisheries in the tropical Pacific: implications for economic development and food security. Clim. Change 119, 199–212, http://dx.doi.org/10.1007/s10584-012-0606-2.

Bell, J.D., Ganachaud, A., Gehrke, P.C., Griffiths, S.P., Hobday, A.J., Hoegh-Guldberg, O., Johnson, J.E., LeBorgne, R., Lehodey, P., Lough, J.M., Matear, R.J., Pickering, T. D., Pratchett, M.S., Sen Gupta, A., Senina, I., Waycott, M., 2013. Mixed responses of tropical Pacific fisheries and aquaculture to climate change. Nat. Clim. Change 3, 519–599. 〈http://dx.doi.org/10.1038/nclimate1838〉.

Bendat, J.S., Piersol, A.G., 1971. Random Data Analysis and Measurement Procedures. Wiley-Interscience, New York.

Bertrand, A., Segura, M., Gutierrez, M., Vasquez, L., 2004. From small-scale habitat loopholes to decadal cycles: a habitat-based hypothesis explaining fluctuation in pelagic fish populations of Peru. Fish Fish. 5, 296–316.

Box, G.E., Jenkins, G.M., 1976. Time Series Analysis: Forecasting and Control. Holden-Day, San Francisco.

Chiodi, A.M., Harrison, D.E., 2010. Characterizing warm-ENSO variability in the equatorial Pacific: an OLR perspective. J. Clim. 23, 2428–2439.

Chiodi, A.M., Harrison, D.E., 2013. El Niño impacts on seasonal U.S. atmospheric circulation, temperature and precipitation anomalies: the OLR-event perspective. J. Clim. 26, 822–837.

Chu, P.-S., Katz, R.W., 1985. Modeling and forecasting the Southern Oscillation: a time-domain approach. J. Clim. 113, 1876–1888.

Chu, P.-S., Katz, R.W., 1989. Spectral estimation from time series models with relevance to the Southern Oscillation. J. Clim. 2, 86–90.

Collins, M., An, S.-I., Cai, W., Ganachaud, A., Guilyardi, E., Jin, F.-F., Jochum, M., Lengaigne, M., Power, S., Timmermann, A., Vecchi, G., Wittenberg, A., 2010. The impact of global warming on the tropical Pacific and El Niño. Nat. Geosci. 3, 391–397, http://dx.doi.org/10.1038/ngeo868.

Diaz, H.F., Hoerling, M.P., Eischeid, J.K., 2001. ENSO variability, teleconnections and climate change. Int. J. Climatol. 21, 1845–1862, http://dx.doi.org/10.1002/joc.631.

Doney, S.C., Ruckelshaus, M., Duffy, J.E., Barry, J.P., Chan, F., English, C.A., Galindo, H.M., Grebmeier, J.M., Hollowed, A.B., Knowlton, N., Polovina, J., Rabalais, N.N., Sydeman, W.J., Talley, L.D., 2012. Climate change impacts on marine ecosystems. Annu. Rev. Mar. Sci. 4, 11–37, http://dx.doi.org/10.1146/annurev-marine-041911-111611.

Ducklow, H.W., Doney, S.C., Steinberg, D.K., 2009. Contributions of long-term research and time-series observations to marine ecology and biogeochemistry. Annu. Rev. Mar. Sci. 1, 279–302.

Ephron, B., Tibshirani, R., 1991. Statistical data analysis in the computer age. Science 253, 390–395.

Fiedler, P.C., 2002. Environmental change in the eastern tropical Pacific Ocean: review of ENSO and decadal variability. Mar. Ecol. Prog. Ser. 244, 265–283.

Ganachaud, A., Sen Gupta, A., Brown, J.N., Evans, K., Maes, C., Muir, L.C., Graham, F. S., 2012. Projected changes in the tropical Pacific Ocean of importance to tuna fisheries. Clim. Change 119, 163–179, http://dx.doi.org/10.1007/s10584-012-0631-1.

Giese, B.S., Ray, S., 2011. El Niño variability in simple ocean data assimilation (SODA), 1871–2008. J. Geophys. Res. 116, C02024, http://dx.doi.org/10.1029/2010/JC006695.

Halpert, M.S., Ropelewski, C.F., 1992. Surface temperature patterns associated with the Southern Oscillation. J. Clim. 5, 577–593.

Harrison, D.E., Chiodi, A.M., 2009. Pre- and post-1997/98 Westerly Wind Events and equatorial Pacific cold tongue warming. J. Clim. 22, 568–581.

Harrison, D.E., Larkin, N.K., 1997. The Darwin sea level pressure record, 1876–1996: evidence for climate change? Geophys. Res. Lett. 24 (14), 1779–1782.

Hughes, C.W., Williams, S.D.P., 2010. The color of sea level: importance of spatial variations in spectral shape for assessing the significance of trends. J. Geophys. Res. 115, C10048, http://dx.doi.org/10.1029/2010JC006102.

Kimura, S., Nakai, M., Sugimoto, T., 1997. Migration of albacore, *Thunus alalunga*, in the North Pacific Ocean in relation to large oceanic phenomena. Fish. Oceanogr. 6 (2), 51–57.

Larkin, N.K., Harrison, D.E., 2002. ENSO warm (El Niño) and cold (La Niña) event life cycles: ocean surface anomaly patterns, their symmetries, asymmetries, and implications. J. Clim., 15; , pp. 1118–1140.

Lehodey, P., Bertignac, M., Hampton, J., Lewis, A., Picaut, J., 1997. El Niño Southern Oscillation and tuna in the western Pacific. Nature 389, 715–718.

Lehodey, P., 2001. The pelagic ecosystem of the tropical Pacific Ocean: dynamic spatial modelling and biological consequences of ENSO. Prog. Oceanogr. 49, 439–468.

Lehodey, P., Chai, F., Hampton, J., 2003. Modelling climate-related variability of tuna populations from a coupled ocean biogeochemical-populations dynamics model. Fish. Oceanogr. 12, 483–494.

Lehodey, P., Alheit, J., Barange, M., Baumgartner, T., Beaugrand, G., Drinkwater, K., Fromentin, J.-M., Hare, S.R., Ottersen, G., Perry, R.I., Roy, C., van der Lingen, C.D., Werner, F., 2006. Climate variability, fish, and fisheries. J. Clim. 19, 5009–5030.

Lehodey, P., Senina, I., Calmettes, B., Hampton, J., Nicol, S., 2012. Modelling the impact of climate change on Pacific skipjack tuna population fisheries. Clim. Change 119, 95–109, http://dx.doi.org/10.1007/s10584-012-0595-1.

Leith, C.E., 1973. The standard error of time-average estimates of climatic means. J. Appl. Meteorol. 12, 1066–1069.

Lu, H.-J., Lee, K.-T., Lin, H.-L., Liao, C.-H., 2001. Spatio-temporal distribution of yellowfin tuna *Thunnus albacores* and bigeye tuna *Thunna obesus* in the tropical Pacific Ocean in relation to large-scale temperature fluctuation during ENSO episodes. Fish. Sci. 67, 1046–1052.

McGowan, J.A., Cayan, D.R., Dorman, L.M., 1998. Climate-ocean variability and ecosystem response in the northeast Pacific. Science 281, 210–217, http://dx.doi.org/10.1126/science.281.5374.210.

Miller, K.A., 2007. Climate variability and tropical tuna: management challenges for highly migratory fish stocks. Mar. Policy 31, 56–70.

Murtugudde, R.G., Signorini, S.R., Christian, J.R., Busalacchi, A.J., McClain, C.R., Picaut, J., 1999. Ocean color variability of the tropical Indo-Pacific basin observed by SeaWiFS during 1997–1998. J. Geophys. Res. 104, 18351–18366, http://dx.doi.org/10.1029/1999JC900135.

Nicholls, N., 2008. Recent trends in the seasonal and temporal behavior of the El Niño-Southern Oscillation. Geophys. Res. Lett. 35, L19703, http://dx.doi.org/10.1029/2008GL034499.

O'Reilly, J.E., Maritorena, S., Mitchell, B.G., Siegel, D.A., Carder, K.L., Garver, S.A., Kahru, M., McClain, C., 1998. Ocean color chlorophyll algorithms for SeaWiFS. J. Geophys. Res. 103 (C11), 24937–24953.

Park, J.-Y., Kug, J.-S., Park, J., Yeh, S.-W., Jang, C.J., 2011. Variability of chlorophyll associated with El Niño-Southern Oscillation and its possible biological

Please cite this article as: Harrison, D.E., Chiodi, A.M., Multi-decadal variability and trends in the El Niño-Southern Oscillation and tropical Pacific fisheries implications. Deep-Sea Res. II (2014), http://dx.doi.org/10.1016/j.dsr2.2013.12.020

feedback in the equatorial Pacific. J. Geophys. Res. 116, C10001, http://dx.doi.org/10.1029/2011JC007056.
Percival, D.B., Walden, A.T., 2000. Wavelet Methods for Time Series Analysis. Cambridge University Press, Cambridge.
Power, S.B., Kociuba, G., 2011. The impact of global warming on the Southern Oscillation Index. Clim. Dyn. 37, 1745–1754.
Power, S.B., Smith, I.N., 2007. Weakening of the Walker Circulation and apparent dominance of El Niño both reach record levels, but has ENSO really changed? Geophys. Res. Lett. 34, L18702, http://dx.doi.org/10.1029/2007GL030854.
Rajagopalan, B., Lall, U., Cane, M.A., 1997. Anomalous ENSO occurrences: an alternate view. J. Clim. 10, 2351–2357.
Rasmusson, E.M., Carpenter, T.H., 1982. Variations in tropical sea surface temperature and surface wind fields associated with the Southern Oscillation/El Niño. Mon. Weather Rev. 110, 354–384.
Ray, S., Giese, B.S., 2012. Historical changes in El Niño and La Niña characteristics in an ocean reanalysis. J. Geophys. Res. 117, C11007, http://dx.doi.org/10.1029/2012JC008031.
Reynolds, R.W., Rayner, N.A., Smith, T.M., Stokes, D.C., Wang, W., 2002. An improved in situ and satellite SST analysis for climate. J. Clim. 15, 1609–1625.
Ropelewski, C.F., Halpert, M.S., 1987. Global and regional scale precipitation patterns associated with the El Niño/Southern Oscillation. Mon. Weather Rev. 115, 1606–1626.
Ropelewski, C.F., Halpert, M.S., 1989. Precipitation patterns associated with the high index phase of the Southern Oscillation. J. Clim. 2, 268–284.
Rossig, J.M., Woodley, C.M., Cech, J.J., Hansen, L.J., 2004. Effects of global climate change on marine and estuarine fishes and fisheries. Rev. Fish Biol. Fish 14, 251–257.
Trenberth, K.E., Hoar, T.J., 1996. The 1990–1995 El Niño-Southern Oscillation event: longest on record. Geophys. Res. Lett. 23, 57–60.
Trenberth, K.E., Hoar, T.J., 1997. El Niño and climate change. Geophys. Res. Lett. 24, 3057–3060.
Troup, A.J., 1965. The 'southern oscillation'. Quart. J. Roy. Meteorol. Soc. 91, 490–506.
Vecchi, G.A., Clement, A., Soden, B.J., 2008. Examining the tropical Pacific's response to global warming. EOS Trans. Am. Geophys. Union 9 (81), 8389 9 (81), 83.
Wittenberg, A.T., 2009. Are historical records sufficient to constrain ENSO simulations? Geophys. Res. Lett. 36, L12702, http://dx.doi.org/10.1029/2009GL038710.
Wunsch, C., 1999. The interpretation of short climate records, with comments on the North Atlantic and Southern Oscillations. Bull. Am. Meterol. Soc. 80, 245–255.

Please cite this article as: Harrison, D.E., Chiodi, A.M., Multi-decadal variability and trends in the El Niño-Southern Oscillation and tropical Pacific fisheries implications. Deep-Sea Res. II (2014), http://dx.doi.org/10.1016/j.dsr2.2013.12.020